



## Larger Ionic Radii Dependent Properties Of $\text{La}^{3+}$ Substituted Co-cu-cr-fe Nanoparticles

Vivek Chaudhari<sup>1</sup>, Sagar E. Shirsath,<sup>2</sup> Maheshkumar L. Mane, R. H. Kadam<sup>4</sup>

<sup>1</sup>D. R. Mane Dr. Babasaheb Ambedkar Marathwada University, Aurangabad 431 001, MS, India

<sup>2</sup>Spin Device Technology Centre, Faculty of Engineering, Shinshu University, Nagano 38-8553, Japan

<sup>3</sup>Department of Physics, SGRG Shinde Mahavidyalaya, Paranda 413502 MS India

<sup>4</sup>Materials Science research lab, Shrikrishna Mahavidyalaya Gunjoti, Osmanabad, MS, India

### Abstract:

*Nanoparticles of  $\text{Co}_{0.7}\text{Cu}_{0.3}\text{Cr}_{0.3}\text{LaFe}_{1.5-x}\text{O}_4$  ( $x = 0.0, 0.025, 0.05, 0.075, 0.1$ ) were synthesized by sol-gel auto combustion method. The synthesized samples were annealed at 600 °C for 4 h. X-ray diffraction data were used to evaluate the structure of the prepared samples. Lattice constant ( $a$ ), X-ray density ( $d_x$ ), jump length ( $L_a$  and  $L_b$ ), allied parameters were calculated using X-ray diffraction data. Lattice constant and X-ray density found to increase with  $\text{La}^{3+}$  substitution. Ion jump lengths and allied parameters are increases with the increase in  $\text{La}^{3+}$  substitution. The variation of all the derived parameters are discussed in the light of difference in the ionic radii of  $\text{La}^{3+}$  ions  $\text{Fe}^{3+}$  ions.*

**Keywords:** Rare earth substitution; Sol-gel method, XRD

### 1.INTRODUCTION

Today, research on, and the manufacturing of, nano-particles with sizes from a few nanometers up to micrometers have been introduced into many different applications including information carriers in biotechnology and medicine. In particular, magnetic nanomaterials represent one of the most exciting prospects in current nanotechnology. Magnetic nanoparticles of ferrites are of great interest in fundamental science, especially for addressing the fundamental relationships between magnetic properties and their crystal chemistry and structure [1].

Cobalt ferrite ( $\text{CoFe}_2\text{O}_4$ ) a well-known hard ferrimagnetic material, in its bulk form crystallizes in mixed spinel structure with space group  $\text{Fd}3\text{m}$ . Mixed copper ferrites are also widely applied in inductors operating at high frequencies because their electrical resistivity is larger than that of magnetic alloys by many orders of magnitude [2]. Thermoelectric power studies of Cu-Cr ferrites as a function of composition and temperature have been studied by Ch. Venkateshwarlu and D. Ravinder [3]. Further, they also investigated thermoelectric power studies of Cu-Co ferrite [4]. Structural, electrical and magnetic properties of Co-Cu ferrite nanoparticles have also been studied by various workers [5].

There are a few reports available which have mentioned the synthesis of rare earth ( $\text{RE}^{3+}$ ) substituted nanocrystalline spinel ferrites in single phase form using different chemical routes despite having big difference in ionic radius of  $\text{RE}^{3+}$  and  $\text{Fe}^{3+}$  ions [6-10].  $\text{R La}^{3+}$  is non-magnetic rare earth cation as it has no 4f electrons [11]. However, its ionic size is much larger than the ionic size of Fe ions.

Please cite this Article as :Vivek Chaudhari, Sagar E. Shirsath,<sup>2</sup> Maheshkumar L. Mane, R. H. Kadam<sup>4</sup>, Larger Ionic Radii Dependent Properties Of  $\text{La}^{3+}$  Substituted Co-cu-cr-fe Nanoparticles : Indian Streams Research Journal (Sept. ; 2012)



So, little amount solid solution of  $\text{La}^{3+}$  in Co-Cu-Cr may create lattice strain in the material and it leads to modify the structure of the spinel ferrite.

To the best of our knowledge there are no reports available on the combination of Co-Cu-Cr ferrite. In this study we made an attempt to study the combination of Co-Cu-Cr ferrite with La substitution.

## 2.EXPERIMENTAL

The ferrite powders were synthesized through a sol-gel auto-combustion route to achieve homogeneous mixing of the chemical constituents on the atomic scale and better sinterability. AR grade cobalt nitrate ( $\text{Co}(\text{NO}_3)_2 \cdot 6\text{H}_2\text{O}$ ), copper nitrate ( $\text{Cu}(\text{NO}_3)_2 \cdot 6\text{H}_2\text{O}$ ), chromium nitrate ( $\text{Cr}(\text{NO}_3)_3 \cdot 9\text{H}_2\text{O}$ ), lanthanum nitrate ( $\text{La}(\text{NO}_3)_3 \cdot 6\text{H}_2\text{O}$ ), iron nitrate ( $\text{Fe}(\text{NO}_3)_3 \cdot 9\text{H}_2\text{O}$ ) and citric acid ( $\text{C}_6\text{H}_8\text{O}_7$ ) were used to prepare the  $\text{Co}_{0.7}\text{Cu}_{0.3}\text{Cr}_{0.5}\text{La}_x\text{Fe}_{1.5-x}\text{O}_4$  ( $x = 0.0, 0.025, 0.05, 0.075, 0.1$ ) ferrite compositions. Reaction procedure was carried out in air atmosphere without protection of inert gases. The molar ratio of metal nitrates to citric acid was taken as 1:3. The metal nitrates were dissolved together in a minimum amount of double distilled water to get a clear solution. An aqueous solution of citric acid was mixed with metal nitrates solution, then ammonia solution was slowly added to adjust the pH at 7. Then the solution was heated at  $90^\circ\text{C}$  to transform into gel. When ignited at any point of the gel, the dried gel burnt in a self-propagating combustion manner until all gels were completely burnt out to form a fluffy loose powder. The auto-ignition of gel was carried out in BOROSIL glass beaker upon a hot plate. The auto-combustion was completed within a minute, yielding the brown-colored ashes termed as a precursor. The as prepared powder then annealed at  $600^\circ\text{C}$  for 4 h. The samples were powdered for X-ray investigations. Part of the powder was X-ray examined by Phillips X-ray diffractometer (Model 3710) using Cu-K radiation ( $\lambda = 1.5405\text{\AA}$ ).

## 3.RESULTS AND DISCUSSION

The annealed ferrites were characterized by XRD. Figure 1 shows the X-ray diffraction pattern of the typical sample  $x = 0.0$ .

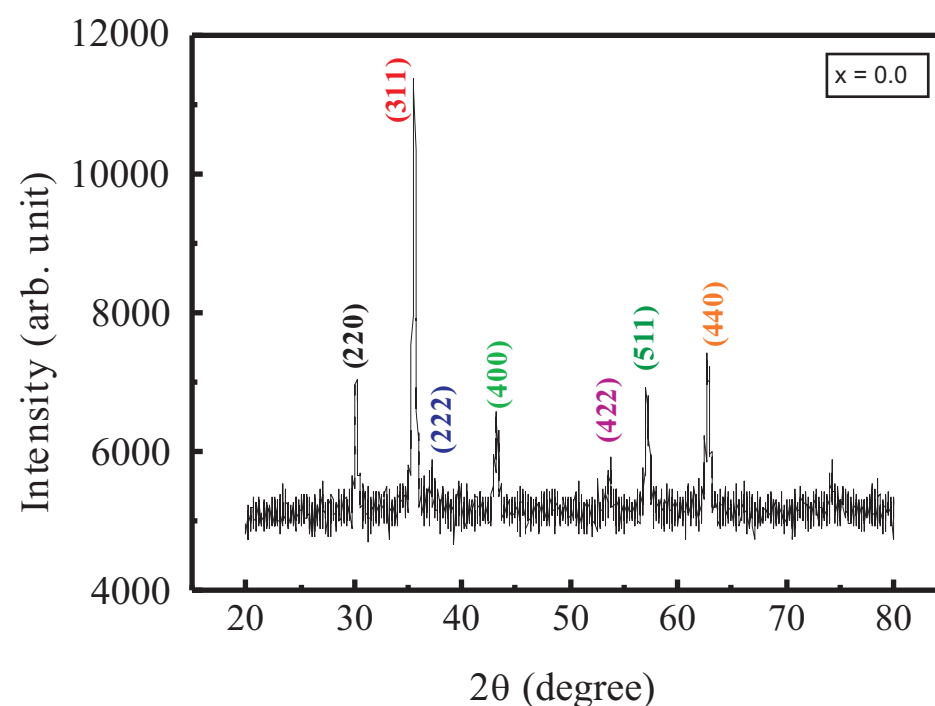
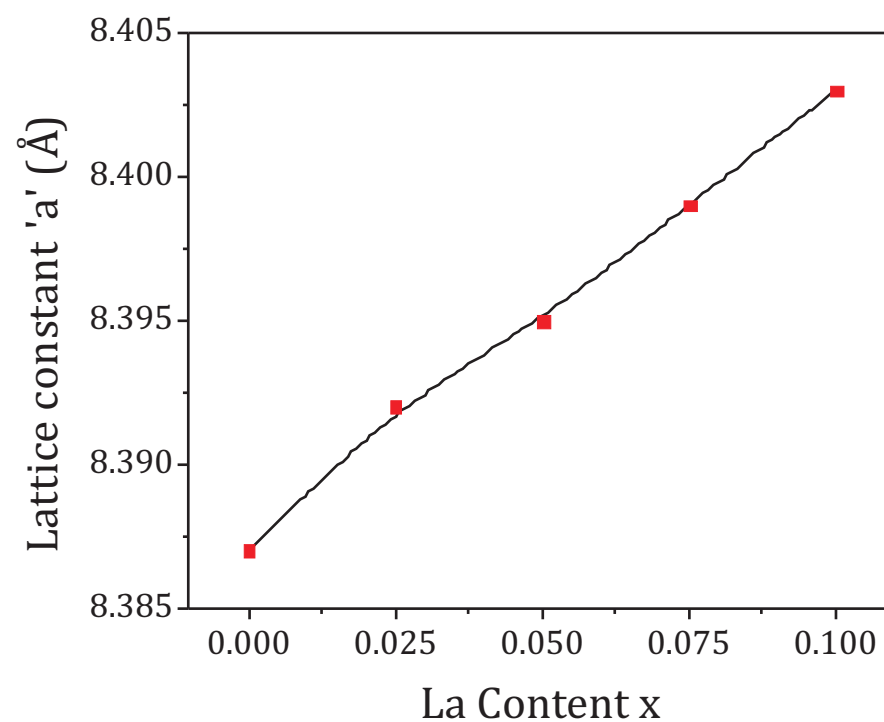


Fig. 1: Typical XRD pattern of  $\text{Co}_{0.7}\text{Cu}_{0.3}\text{Cr}_{0.5}\text{La}_x\text{Fe}_{1.5-x}\text{O}_4$

The lattice parameter 'a' was calculated using the following equation [12],

$$a = d \sqrt{h^2 + k^2 + l^2}$$

where  $d$  is the inter-planer spacing and  $(hkl)$  is the index of the XRD reflection peak.



**Fig. 2:** Variation of lattice constant with  $\text{La}^{3+}$  substitution of  $\text{Co}_7\text{Cu}_{0.3}\text{Cr}_{0.5}\text{La}_x\text{Fe}_{1.5-x}\text{O}_4$

It is observed from Fig. 2 that lattice constant 'a' increases from 8.387- 8.403 Å with increase in  $\text{La}^{3+}$  substitution. In the present ferrite system smaller  $\text{La}^{3+}$  with larger ionic radii (1.05 Å) substituted for  $\text{Fe}^{3+}$  ions of smaller ionic radii (0.67 Å). This difference in ionic radii is reflected in the variation of lattice constant (Fig. 2).

The X-ray density ( $d_x$ ) of all the samples of the series was obtained by the following relation.

$$d_x = \frac{8M}{Na^3}$$

where 8 is the number of molecules per unit cell, 'M' is the molecular weight of sample, 'N' is the Avogadro's number and 'a' is lattice constant. It was noted that the X-ray density increases from 5.269 to 5.424 g/cm<sup>3</sup> with increase in  $\text{La}^{3+}$  substitution. This behaviour of X-ray density is related to the molecular weight (M) and lattice constant (a). In the present work, molecular weight increases with increase in  $\text{La}^{3+}$  substitution, this result in the increase in X-ray density of the samples for  $\text{La}^{3+}$  substitution.

The average crystallite diameter 'D<sub>XRD</sub>' of powder estimated from the most intense (311) peak of XRD and using the Scherrer formula[13],

$$D_{XRD} = \frac{0.9\lambda}{B \cos\theta}$$

where  $\lambda$  is the wavelength used in XRD, B is the full width of half maximum in (2 $\theta$ ), is the corresponding Bragg angle. Figure 3 shows that the crystallite diameter decreases from 25 to 15 nm with increase in  $\text{La}^{3+}$  substitution.

The specific surface area (S) was calculated from the diameter of the particle in nanometer and the measured density in g/cm<sup>3</sup> using the relation [14],

$$S \propto \frac{6000}{Dd_B}$$

where D is the average crystallite size and dB is the bulk density. The variation of surface area (S) with La content x is shown in Fig. 3. The specific surface area goes on increasing with increase in La substitution. The increase in S is associated with increase in crystallite size.

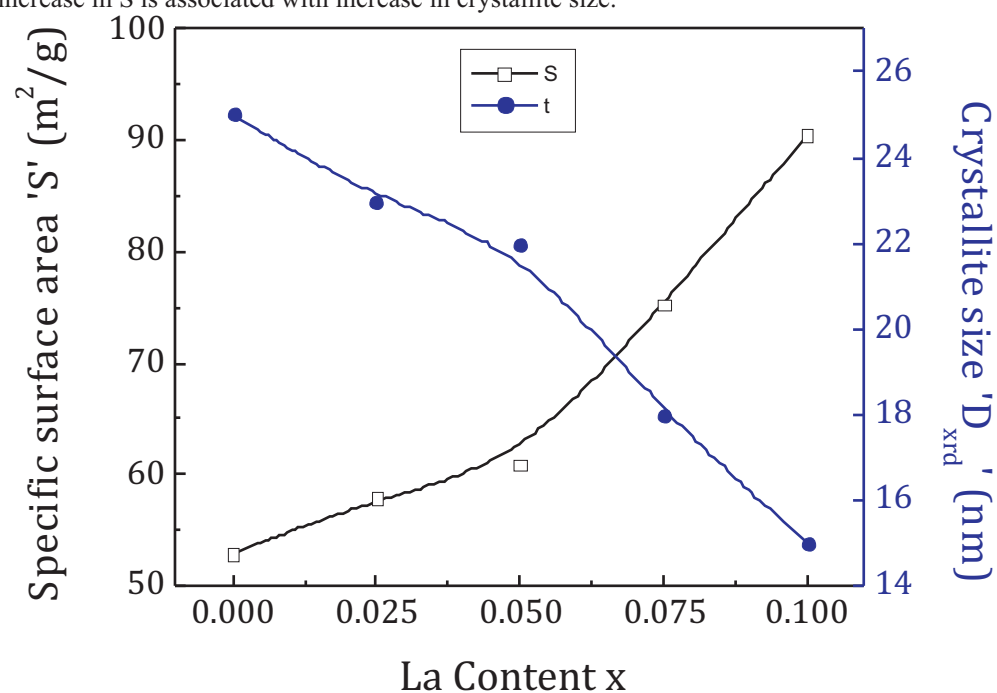


Fig. 3: Variation of specific surface area (S) and crystallite size (D<sub>xrd</sub>) with La substitution of Co<sub>0.7</sub>Cu<sub>0.3</sub>Cr<sub>0.5</sub>La<sub>x</sub>Fe<sub>1.5-x</sub>O<sub>4</sub>

The ion jump length for tetrahedral A-site (L<sub>A</sub>) and octahedral B-site (L<sub>B</sub>) are calculated using the following relations,

$$L_A \propto a\sqrt{\frac{3}{4}}$$

$$L_B \propto a\sqrt{\frac{2}{4}}$$

Fig. 4 shows the variation of ion jump lengths with La substitution. It is observed from Fig. 4 that the jump length of ions at tetrahedral A and octahedral B site is increases with increase in La substitution. This behavior of ion jump length with La substitution is related with the variation of lattice constant with La<sup>3+</sup> substitution. This variation in L<sub>A</sub> and L<sub>B</sub> is attributed to the deference in the ionic radii of the La<sup>3+</sup> and Fe<sup>3+</sup> ions. As the La<sup>3+</sup> substitution increases, they increase the distance between magnetic ions and consequently the ion jump lengths increases.

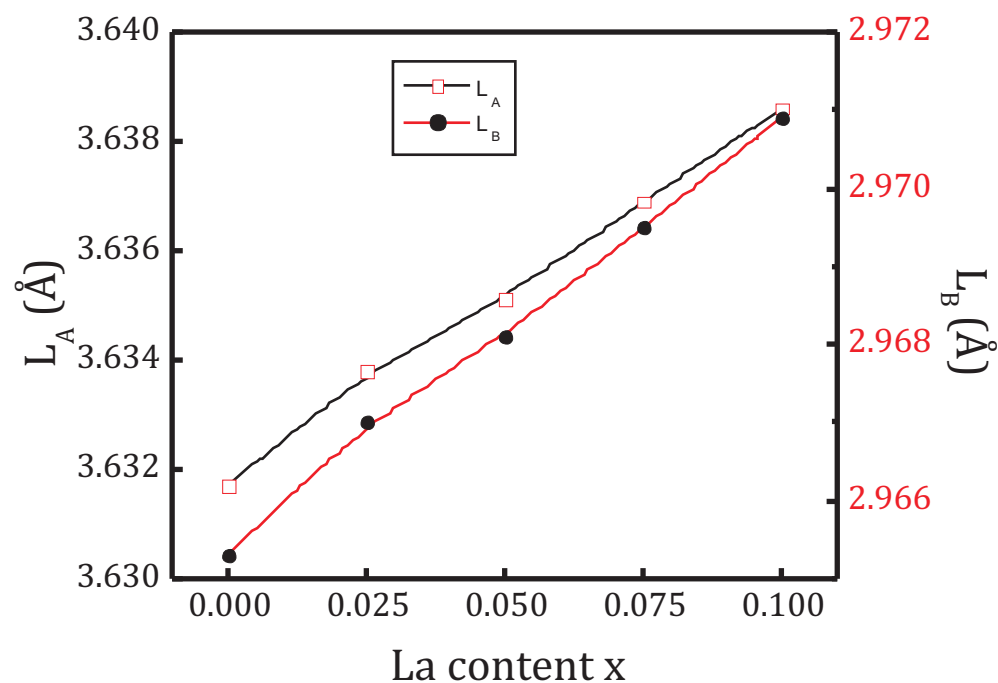


Fig. 4: Variation of ion jump lengths (LA and LB) with La substitution of of  $C_6Cu_{0.3}Cr_{0.5}La_xFe_{1.5-x}O_4$ .

Using the experimental values of lattice constant 'a', oxygen positional parameter 'u' (0.375 Å) and substituting using the following equations, the allied parameters such as tetrahedral and octahedral bond length (dAx and dBx), tetrahedral edge, shared and unshared octahedral edge (dAXE, dBXE and dBXEU) were calculated.

$$d_{Ax} = a \theta 3 (u-1/4) \quad 7$$

$$d_{Bx} = a [3u^2 - (11/4)u + 43/64]^{1/2} \quad 8$$

$$d_{AxE} = a \theta 2 (2u-1/2) \quad 9$$

$$d_{BxE} = a \theta 2 (1-2u) \quad 10$$

$$d_{BxEu} = a [4u^2 - 3u + (11/16)]^{1/2} \quad 11$$

Figure 5 show that all the allied parameter increases with the increase in  $La^{3+}$  substitution. The variation of allied parameters is related to the difference in the ionic radii of  $La^{3+}$  and  $Fe^{3+}$ . The  $La^{3+}$  ion with the larger ionic radii increases the allied parameter as the replaces  $Fe^{3+}$  ions of smaller ionic radii.

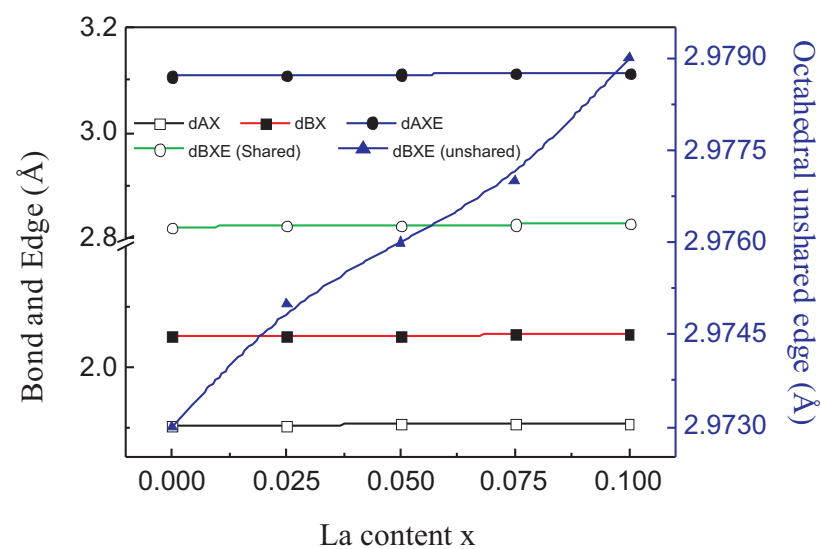


Fig. 5. Variation of Tetrahedral bond (dAX), octahedral bond (dBX), tetra edge (dAXE) and octahedral edge (dBXE) (shared and unshared) with La content x of  $\text{Co}_{0.7}\text{Cu}_{0.3}\text{Cr}_{0.5}\text{La}_x\text{Fe}_{1.5-x}\text{O}_4$

## 1.CONCLUSIONS

$\text{La}^{3+}$  substituted Co-Cu-Cr ferrites nanoparticles with a chemical formula  $\text{Co}_{0.7}\text{Cu}_{0.3}\text{Cr}_{0.5}\text{La}_x\text{Fe}_{1.5-x}\text{O}_4$  were successfully synthesized via the sol-gel method. Lattice constant and X-ray density found to increase with the increase in  $\text{La}^{3+}$  ions, this increase in a and dx is related to ionic radii and molecular weight of  $\text{La}^{3+}$  ions. The average crystallite size decreases with increase in  $\text{La}^{3+}$  substitution result in increase in specific surface area of the particles. Ion jump length of tetrahedral A- and octahedral B-sites increases with the increase  $\text{La}^{3+}$  substitution. All the allied parameters show increasing trend with the increase in  $\text{La}^{3+}$  substitution. This behaviour of ion jump lengths and allied parameters are related to the larger ionic radii of  $\text{La}^{3+}$  ions as compared to that of  $\text{Fe}^{3+}$  ions.

## REFERENCES

- [1] Alex Goldman, Modern Ferrite Technology, 2nd ed. (Springer, New York, 2006).
- [2] Zhongbing Huang, Guangfu Yin, Xiaoming Liao, Yadong Yao, Yunqing Kang, J. Coll. Inter. Sci. 317 (2008) 530
- [3] Ch. Venkateswarlu and D. Ravinder, J. Alloy. Compd. 397 (2005) 5.
- [4] Ch. Venkateswarlu and D. Ravinder, J. Alloy. Compd. 426 (2006) 4.
- [5] Mohd. Hashim, Alimuddin, Shalendra Kumar, B.H. Koo, Sagar E. Shirsath, E.M. Mohammed, Jyoti Shah, R.K. Kotnala, H.K. Choi, H. Chung, Ravi Kumar, J. Alloy. Compd. 518 (2012) 11.
- [6] L. Myrtil, Z. Kahn, John Zhang, Appl. Phys. Lett. 78 (2001) 3651–3654.
- [7] R.N. Panda, J.C. Shih, T.S. Chin, J. Magn. Magn. Mater. 257 (2003) 79–86.
- [8] L. Zhao, Y. Cui, H. Yang, L. Yu, W. Jin, S. Feng, Mater. Lett. 60 (2006) 104–108.
- [9] W.C. Kim, S.J. Kim, J.C. Sur, C.S. Kim, J. Magn. Magn. Mater. 242 (2002) 197–200.
- [10] L.B. Tahar, M. Artus, S. Ammar, L.S. Smiri, F. Herbst, M.J. Vaulay, V. Richard, J.M. Greneche, F. Villian, F. Fievet, J. Magn. Magn. Mater. 320 (2008) 3242–3250.
- [11] R. Valenzuela, Magnetic Ceramics, Cambridge University Press, 1994.
- [12] B. D. Cullity, Elements of X-ray diffraction, (Addison-Wesley, London, 1959)
- [13] C. Caizer and M. Stefanescu, J. Phys. D. Appl. Phys. 35 (2002) 3035.
- [14] I. H. Gul, A. Z. Abbasi, F. Amin, M. Anis-Ur Rehman, A. Maqsood, J. Magn. Magn. Mater. 311 (2007) 494.